Biosensors and Bioelectronics 54 (2014) 421–427

Contents lists available at ScienceDirect

Biosensors and Bioelectronics

journal homepage: www.elsevier.com/locate/bios

3D printed chip for electrochemical detection of influenza virus labeled with CdS quantum dots

Ludmila Krejcova [a], Lukas Nejdl [a], Miguel Angel Merlos Rodrigo [a,b], Michal Zurek [a], Miroslav Matousek [a], David Hynek [a,b], Ondrej Zitka [a,b], Pavel Kopel [a,b], Vojtech Adam [a,b], Rene Kizek [a,b,*]

[a] Department of Chemistry and Biochemistry, Faculty of Agronomy, Mendel University in Brno, Zemedelska 1, 613 00 Brno, Czech Republic
[b] Central European Institute of Technology, Brno University of Technology, Technicka 3058/10, 61600 Brno, Czech Republic

ARTICLE INFO

Article history:
Received 17 August 2013
Received in revised form
10 October 2013
Accepted 21 October 2013
Available online 1 November 2013

Keywords:
3D Printing
Microfluidic chip
Voltammetry
Paramagnetic particles
Influenza hemagglutinin
Quantum dots

ABSTRACT

In this study, we report a new three-dimensional (3D), bead-based microfluidic chip developed for rapid, sensitive and specific detection of influenza hemagglutinin. The principle of microfluidic chip is based on implementation of two-step procedure that includes isolation based on paramagnetic beads and electrochemical detection. As a platform for isolation process, streptavidin-modified MPs, which were conjugated via biotinylated glycan (through streptavidin–biotin affinity) followed by linkage of hemagglutinin to glycan, were used. Vaccine hemagglutinin (HA vaxi) was labeled with CdS quantum dots (QDs) at first. Detection of the isolation product by voltammetry was the end point of the procedure. The suggested and developed method can be used also for detection of other specific substances that are important for control, diagnosis or therapy of infectious diseases.

1. Introduction

Influenza is likely the most powerful member of the group of potential pandemic agents (Krasnoselsky and Katze, 2012), because of the continuous mutational changes in its surface antigens, hemagglutinin (HA) and neuraminidase (NA), which play the main role in the mechanism of their interaction with sialic acid (SA) receptors on a host cell (Chen et al., 2013).

Numerous analytical methods are used to detect influenza viruses including methods based on the direct isolation of viruses (Bui et al., 2013) followed by real time-polymerase chain reaction (RT-PCR) (Tong et al., 2012), or immunology tests (Hemmatzadeh et al., 2013; Shembekar et al., 2013). Most of them have some disadvantages (an isolation of virus is time consuming; RT-PCR requires appropriate equipment and well-trained staff). For this reason, new sensors and biosensors based on magnetic beads separation are coming to the forefront (Kamikawa et al., 2010; Lien et al., 2011). Its sensitivity, specificity, speed, and the ability to recognize a very low concentration of target molecules belong to the most important features of a biosensor (Xu and Wang, 2012). For this reason, wide range of methods, materials and substances to optimize developing biosensing instrument has been tested (Kim et al., 2013). Paramagnetic particles (MPs) are the excellent tool with many advantageous features, such as easy handling and possibility to be separated by the magnetic field (Gijs, 2004; Ramadan and Gijs, 2012). Currently, various bead-based assays implemented to microfluidic systems have been reported for biomedical applications (Lien et al., 2011; Tsai et al., 2013). Combination of advanced biological detection methods with microfluidic and immunomagnetic separation techniques exploiting functionalized magnetic particles has tremendous potential for realization of an integrated system for detection of pathogens (Casavant et al., 2013; Ramadan and Gijs, 2012).

In this study, the microfluidic assay based on MPs based isolation of HA was followed with the indirect detection of the isolated compound with QDs labels. Microfluidic device for isolation and detection of HA–QDs was fabricated using three-dimensional (3D) printing, which is an example of additive manufacturing or solid freeform fabrication technology (Polzin et al., 2013).

2. Experimental section

2.1. Chemicals

Streptavidin Dynabeads M-270 was purchased from Life Technologies (Norway), uniform and superparamagnetic beads are

* Corresponding author at: Mendel University in Brno, Department of Chemistry and Biochemistry, Faculty of Agronomy, Zemedelska 1, 613 00 Brno, Czech Republic. Tel.: +420 5 4513 3350; fax: +420 5 4521 2044.
E-mail address: kizek@sci.muni.cz (R. Kizek).

0956-5663/$ - see front matter © 2013 Elsevier B.V. All rights reserved.
http://dx.doi.org/10.1016/j.bios.2013.10.031

2.8 μm in diameter, with a monolayer of recombinant streptavidin covalently coupled to the surface. Biotinylated multivalent-glycan (01-039a [Neu5Acα2–6 Galβ1–4GlcNAcβ1-PAA-biotin]) from GlycoTech (USA), Vaxigrip® (HA) from Sanofi Pasteur (France), and tris(2-carboxyethyl)phosphine (TCEP) from Molecular Probes (USA). Sample of inactivated influenza H5N1 was donated by University of Veterinary and Pharmaceutical Sciences Brno. $Co(NH_3)_6Cl_3$ and other chemicals were purchased from Sigma Aldrich (USA) in ACS purity unless indicated otherwise. Stock solutions were prepared with ACS water. pH value was measured using an instrument inoLab Level 3 (Wissenschaftlich-Technische Werkstatten GmbH; Germany). Deionised water underwent demineralization by reverse osmosis using an apparatus Aqua Osmotic 02 (Aqua Osmotic, Czech Republic) and was subsequently purified using Millipore RG (Millipore Corp., USA). Deionised water was used for rinsing, washing, and preparation of buffers.

2.2. Hemagglutinin

Influenza vaccine Vaxigrip®, which contains inactivated and split influenza virions of the following strands: A/California/7/2009 (H1N1), A/Victoria/361/2011 (H3N2) and B/Wisconsin/1/2010, was used as the sample of Influenza A and B hemagglutinin. Vaxigrip contains 15 micrograms of all three HA per 0.5 mL (together 90 μg/mL HA).

2.3. Preparation of QDs (CdS)

CdS quantum dots were prepared according to modified previously published protocol (Li et al., 2007). Briefly, cadmium nitrate tetrahydrate $Cd(NO_3)_2 \cdot 4H_2O$ (0.1 mM) was dissolved in ACS water (25 ml). 3-mercaptopropionic acid (35 μL, 0.4 mM) was slowly added to the stirred solution. Afterwards, the pH was adjusted to 9.11 with 1 M NH_3 (1.5 mL). Sodium sulfide nonahydrate $Na_2S \cdot 9H_2O$ (0.1 mM) in ACS water was poured into the solution under vigorous stirring. The acquired yellow solution was stirred for 1 h. Prepared CdS quantum dots were stored in the dark at 4 °C and were used for labeling of HA.

2.4. Labeling of HA from Vaxigrip by QDs (CdS)

Two preparation procedures of HA–CdS complex were designed. The effect of complex fabrication was tested using an automatic isolation procedure (described in Section 2.6) with subsequent electrochemical detection using hanging mercury drop electrode (described in Section 2.7).

Procedure No. 1: Vaxigrip® (0.5 mL, containing 15 μg of H1N1, H3N2 and Brisbane virions) was mixed with QDs (0.5 mL) and shaken for 16 h in dark at room temperature on a Biosan OS-10 Orbital Shaker (Biosan Ltd., Latvia). Dialysis of the sample was performed on a Millipore filter 0.025 μm VSWP against 2 L of miliQ water at 4 °C. During dialysis volume of sample increased to 4.5 mL. Volume was reduced to 1 mL on an Amicon 3k on centrifuge 5417R (Eppendorf, Germany) at 6000 rpm for 15 min at 20 °C. Concentrations of HA and QDs (expressed as Cd content) were as it follows: 3 × 15 μg HA and 115 μg Cd/mL.

Procedure No. 2: Vaxigrip (500 μL) was reduced and washed with water (5 × 400 μL) on an Amicon 3k centrifugal filter device (Millipore, USA) and mixed with a solution of prepared QDs (500 μL). This mixture was shaken for 24 h at room temperature on a Biosan Orbital Shaker OS-10. The volume of solution was reduced to 100 μL on an Amicon Ultra 3k, diluted with water and washed 5 times using centrifuge 5417R. The washed sample was diluted to 1 mL and used for succeeding measurements. Concentrations of HA and QDs were the same as in the case of *Procedure no.* 1.

2.5. Characterization of vaxi HA, CdS and HA–CdS isolated by MPs

Characterization of vaxi HA, CdS and HA–CdS complex were provided by matrix-assisted laser desorption/ionization time of flight mass spectrometry (MALDI-TOF MS), gel electrophoresis and spectral analysis. MPs and HA–CdS complex isolated by MPs were characterized also by scanning electrochemical microscope (SCEM).

2.5.1. Characterization of vaxi HA, CdS and HA–CdS complex by spectral analysis

Fluorescence and/or absorption spectra of vaxi HA, CdS and HA–CdS were acquired by a multifunctional microplate reader Tecan Infinite 200 PRO (TECAN, Switzerland). 230, 320, 430, 450 and 550 nm were used as excitation wavelengths and the fluorescence scan was measured within the range from 290 to 850 nm per 5 nm steps. The detector gain was set to 100. Absorption scan was measured within the range from 230 to 630 nm. Samples (50 μL) were placed in UV-transparent 96 well microplate with flat bottom by CoStar (Corning, USA). All measurements were performed at 30 °C and controlled by a Tecan Infinite 200 PRO.

2.5.2. Characterization of vaxi HA by MALDI-TOF MS

The mass spectrometry characterization was performed by MALDI-TOF/TOF mass spectrometer Bruker Ultraflextreme (Bruker Daltonik GmbH, Germany) equipped with a laser operating with wavelength of 355 nm according to Nejdl et al. (in press).

2.5.3. Characterization of vaxi HA by gel electrophoresis

Sodium dodecyl sulfate polyacrylamide gel electrophoresis (SDS-PAGE) was performed using a Mini Protean Tetra apparatus with gel dimension of 8.3 × 7.3 cm^2 (Bio-Rad, USA) according to Vyslouzilova et al. (2013).

2.5.4. Characterization of MPs and MPs–glycan–HA–CdS by SECM

Characterization of MPs and MPs–glycan–HA–CdS was provided by SECM at CH Instruments Scanning electrochemical microscope 920C (Metrohm, Switzerland) in Amperometric mode. Working electrode was a disk shaped microelectrode with radius of the conductive core 10 μm. The dimensionless parameter RG defined as ratio of radii of conductive and isolated cores was 5.4. The following parameters were used for working and substrate electrode: WE (working electrode, Pt); applied potential: 0.3V, SA (substrate electrode, Au): applied potential −0.4 V Ferrocenemethanol concentration 1 mM was used as an electrochemical mediator. All the experiments were done at the same distance between tip and substrate (d = 30 μm).

The electrochemical cell was cleaned ultrasonically (in the mixture of acetone and ethanol in the same ratio) and furthermore was purified with hydrogen peroxide and sulfuric acid (also in the same ratio). The purification step took five minutes on the surface of electrode to purify it. The tip was cleaned ultrasonically only in ethanol. Afterwards the chemical cleaning was finished, when the cyclic voltammetry (CV) was started in the presence of 30% (v/v) sulfuric acid. Finally, all the above-mentioned parts were rinsed with double distilled water and dried with nitrogen. This procedure was repeated after each measurement. Firstly, electrochemical mediator (ferrocenemethanol with KCl in ratio 1:1) was identified. CV was initiated to determine what potential is responsible for reversible redox reaction of mediator. These potentials were applied to reach approach curves– determination of optimal tip–substrate distance (30 μm). The bare substrate electrode was scanned and after it MPs and MPs–HA–CdS were scanned too.

2.6. Isolation of HA-QDs by MPs modified with glycan using robotic pipetting station

A computer-controlled automated pipetting station, *ep-Motion* 5075 (Eppendorf) was used for automated sample handling prior to electrochemical analysis. Position C1 was thermostated (Epthermoadapter PCR96). After the separation, MPs were forced apart using a Promega magnetic pad (Promega, USA) at position C4. The program sequence was edited and the station was controlled with pEditor 4.0. Pipetting of 10 μL of streptavidin Dynabeads M-270 to microplates (PCR 96, Eppendorf) was the first step of isolation process. Subsequently, plate was transferred to magnet. Stored solution was aspirated from the MPs and MPs were washed three times with 100 μL of phosphate buffer (PB) (0.3 M, pH 7.4, made from NaH_2PO_4 and Na_2HPO_4). Thereafter volume of 20 μL of biotinylated glycan was added to each of the wells and incubated (30 min, 25 °C, 400 rpm). After the incubation, the sample was washed three times with PB (0.3 M, pH 7.4). Subsequently 20 μL of HA-QDs was added. Mixture in each well was further incubated (400 rpm, time and temperature was optimized) and washed three-times with 100 μL of PB (0.3 M, pH 7.4). In the last step, 35 μL of PB (0.3 M, pH 7.4) was added. This step was followed by the treatment of a sample using ultrasound needle (2 min). The plate was transferred to the magnet and the supernatant was analyzed using voltammetry. The detected substance was identified as cadmium (CdS QDs) and protein (HA from Vaxigrip).

2.7. Electrochemical analysis of HA–CdS isolated by robotic pipetting station

For electrochemical analysis of both parts of isolated HA–CdS complex two different techniques and supporting electrolytes were applied.

2.7.1. Determination of vaxi HA from HA–CdS complex by Brdicka reaction

Adsorptive transfer technique differential pulse voltammetric measurements (AdT DPV) were performed with a 663 VA Stand instrument (Metrohm, Switzerland) according to experimental conditions indicated by Sochor et al. (2012).

2.7.2. Determination of cadmium from HA–QDs complex in acetate buffer

Determination of cadmium by differential pulse anodic stripping voltammetry (DPASV) was performed using a 663 VA Stand (Metrohm, Switzerland) and a standard cell with three electrodes according to experimental conditions indicated by Krejcova et al. (2012).

2.8. Fabrication of 3D microfluidic chip and its application

The first step in fabrication of microfluidic chip was its 3D processing in the modeling program Blender 2.65 (available on the http://www.blender.org/community/get-involved). Product of this software was exported in STL format and further edited in netFabb program (Parsberg, Germany), which allows elimination of cranny or wrongly oriented triangles. The corrected model (in STL format) was opened in the program G3DMAKER (DO-IT, Czech Republic) and 3D printing was controlled by EASY 3D MAKER (DO-IT). After the above-mentioned corrections, the model was ready for printing. Chip of the size [x, y and z] 42.64/14.95 and 4.87 mm was printed with an accuracy of [x, y and z] 0.1/0.1 and 0.08 mm for 94 min. As material polylactide (PLA) from DO-IT, which was applied by extrusion (melting head) at temperature 210 °C on a heated surface (40 °C), was used. Each printed chip was machined from minor impurities, fitted with tubes with a diameter of 2.1 mm and with three electrodes (working glassy carbon microelectrode, reference graphite electrode and auxiliary platinum wire) for detail description see Section 2.8.2. Attachment the plastic film (thickness 0.7 mm) at top of chip was the last step of procedure.

2.8.1. Microfluidic analysis

A microfluidic analysis system (3D chip) equipped with devices for electrochemical detection was suggested and constructed. Procedure included two basic steps: isolation and electrochemical detection. Isolation procedure was based on glycan conjugated MPs, which was used for binding of HA (vaccination or real sample) labeled by QDs (Fig. S2, Part 1). The isolation procedure was done as it follows: 10 μL of MPs was dosed by a peristaltic pump (Pump Amersham Biosciences, Sweden). Using an external magnet it was anchored on the reaction chamber, stored solution from the MPs was aspirated and MPs were washed with 1500 μL of PB. Thereafter, MPs were modified with 20 μL of biotinyled Glycan (50 μg/mL). This step was followed by washing with 1500 μl of PB. The last part of the isolation was binding of HA–CdS (20 μL, concentration 45 μg/mL) onto glycan-modified MPs, again followed by a washing with 1500 μL of PB. After it, chip with MPs-glycan-HA–CdS was immersed in an ultrasonic bath and MPs–glycan–HA–CdS complex was fractionated. Isolated HA was detected indirectly due to electroactivity of Cd(II), respectively CdS in the isolated HA–CdS complex.

2.8.2. Electrochemical detection of the isolated HA–CdS complex by glassy carbon microelectrode

Measurements were carried out using three-electrode set up. As the working electrode a glassy carbon microelectrode (GCm) was used, as the quasi-reference electrode a graphite lead was used and as the auxiliary electrode a platinum electrode with diameter 0.5 mm (CH Instruments, USA) was used. GCm was purchased from (Sensolytics, Germany). The pencil leads (diameter = 500 μm, length = 60 mm) were purchased from Koh-I-Noor (Czech Republic). Immersing 3 mm of the pencil lead into a solution resulted in an active electrode area of 4.91 mm^2. The electrodes were used without any pre-treatments except GCm, which was polished by 0.3 m polishing paper.

The differential pulse voltammetry (DPV) was used as the measuring method for detection of cadmium part of the complex under the following parameters: initial potential −1.3 V, end potential −0.1 V, deposition potential −1.3 V, deposition time 85 s, modulation amplitude 0.1 V, step potential 0.005 V, scan rate 0.05 V/s. Acetate buffer (0.2 M, pH 5) was used as the supporting electrolyte. The experiments were carried out at 20 °C. The electrochemical signal was detected by PGSTAT101 Autolab potentiostat (Metrohm, The Netherlands) and the results were evaluated by the Software NOVA 1.8 (Metrohm). The cadmium signal was detected at potential −0.9 V.

2.9. Descriptive statistics

Data were processed using MICROSOFT EXCELs (USA) and STATISTICA.CZ Version 8.0 (Czech Republic). The results are expressed as mean ± SD unless noted otherwise. The detection limits (3 signal/noise, S/N) were calculated according to Long and Winefordner (1983).

3. Results and discussion

Influenza A surface antigen, hemagglutinin, occurs in different host specific subtypes, which binds human and/or avian type

receptors with high specificity (Stevens et al., 2006). Those highly specific affinities of HA-receptors were utilized as a basic pattern for isolation of various types of influenza viruses (Suenaga et al., 2012). In our previous study a biosensor for influenza detection was designed. It consists from automatic MPs-based isolation process of standard viral protein modified with CdS QDs with subsequent electrochemical detection of HA (direct detection of virus) and QDs (indirect detection of virus) (Krejcova et al., 2012). This study is based on the previously published concept, but the main idea was to develop 3D fabricated microfluidic chip and applied it for analysis of a real sample (vaxi HA). Primarily, we focused on the designing and implementation of the method for isolation and detection of HA–CdS by magnetic field controllable microfluidic 3D chip. The isolation was stable due to the continual washing process at a flow rate of 480 μL/min. The flow was discontinued in two isolation steps: (i) conjugation of glycan on MPs surface and (ii) conjugation of HA–CdS on surface of glycan-modified MPs. Under these conditions, the isolation process was very specific because non-specifically bounded substances were eliminated by the washing process compared to stationary measurements. The beads-based isolation of HA–CdS complex was the cornerstone of the procedure. Glycan-conjugated (modified) beads bound vaccine HAs, which could be recognized specifically and linked onto the surface of the glycan-modified MPs.

In the first step, different method for characterization of reactants (spectral analysis, matrix-assisted laser desorption/ionization time of flight mass spectrometry, gel electrophoresis, scanning electrochemical microscope) were used.

3.1. Characterization of reactant by different method

3.1.1. Spectral characterization of vaxi HA, CdS, and HA–CdS complex

In this section, we focused on UV/VIS and fluorescence spectrometric characterization of HA–CdS complex. Spectral characteristics of nanoparticles hold a special place among properties of these materials. Differences (sometimes very considerable) between compact semiconductor materials and the corresponding nanoparticles are the most distinct in this context, and a theoretical basis was created to interpret many of the observed effects (Shalyapina et al., 2013). The first recorded absorption scan of CdS showed the absorption maximum at $\lambda = 450$ nm (Fig. S1A and a). Formation of the HA–CdS complex resulted in a change in absorption spectrum and in a decrease of the absorption maximum, as shown in Fig. S1A and b. The absorption maximum was not observed in the case of HA (Fig. S1A and c). Furthermore, the fluorescence intensities of CdS (Fig. S1B) and HA–CdS (Fig. S1C) complexes were compared, whereas different excitation wavelength were tested ($\lambda = 230$, 320, 430, 450, and 550 nm). The highest intensity of fluorescence was observed at $\lambda = 430$ nm (Fig. S1B and e). Formation of HA–CdS complex was reflected by a decrease in fluorescence by 25 % on the average (Fig. S1C and e). Differences between water, CdS, and HA–CdS complex were also visualized by UV and are shown in Fig. S1D.

3.1.2. Characterization of influenza vaccine by matrix-assisted laser desorption/ionization time of flight mass spectrometry and gel electrophoresis

After that we characterized the spectral properties of the complexes used in this study, we followed with their further characterization, mainly, with characterization of isolation design. The beads-based isolation of HA–CdS complex was the cornerstone of the procedure. Glycan-conjugated (modified) beads bound vaccine HAs, which could be recognized specifically and linked onto the surface of the glycan-modified MPs (Fig. S2/Part 1). This design is based on the hemagglutinin as the basic element. Therefore, the protein characterization of influenza vaccine by MALDI-TOF MS and gel electrophoresis was the further key step.

MALDI-TOF MS was used to characterize vaccine (Vaxigrip) mass spectra. Vaccine consists of three influenza's HAs (A/California/7/2009 (H1N1), A/Victoria/361/2011 (H3N2) and B/Wisconsin/1/2010), which were cultivated on embryonated eggs, concentrated, purified by zone centrifugation in a sucrose gradient, split, inactivated, and then diluted in phosphate buffered saline solution. The MALDI-TOF spectra showed three distinct peaks corresponding to vaccine HAs as indicated by the manufacturer. Fig. S2/Part 2 shows the detected proteins in the spectra of vaccine represented by three peaks (28 000 m/z, 48 000 m/z and 56 000 m/z). These results were compared with the SDS-PAGE gel (showed in insert in Fig. S2/Part 2) and the comparison brings the identical results, which is in good agreement with the published data (Epand and Epand, 2002; Garcia-Canas et al., 2010; Schwarzer et al., 2009). The proportions of several influenza proteins were found to be similar for various strains of the virus (Epand and Epand, 2002). One peak at 28 kDa corresponds to the matrix protein 1 (M1). The peak at 38 kDa represents the hemagglutinin fragment from influenza B virus. The peak at 48 kDa was assigned to the glycosylated HA (Chou et al., 2011). The highest peak in MALDI-TOF record at 56 kDa is connected with the presence of nucleocapsid protein (NP). The HA peak is necessary to search for at 63 kDa. This peak was also detected as expected (Fig. S2/Part 2).

3.1.3. Characterization of MPs–HA–CdS complex by scanning electrochemical microscope

It clearly follows from the obtained results that we successfully characterized all materials need for construction of beads-based isolation of virus. As further step, verification of MPs binding to HA–CdS was performed. SECM was used to characterize the MPs itself and HA–CdS complex bounded to MPs modified by glycan. Scan of the structure of the sample is performed in the SECM conventional feedback mode. Fig. S2/Part 3A shows the SECM images of MPs itself and Fig. S2/Part 2B shows MPs–glycan–HA–CdS complex formed during the isolation procedure. Current level of MPs itself was −0.6 nA, current level of the MPs–glycan–HA–CdS complex was −0.45 nA. Differences between current levels of both samples are caused by the formation of MPs–HA–CdS complex, because the presence of cadmium(II) enables to increase the level of current.

3.2. Optimization of the isolation procedure in stationary design connected with HMDE detection

Various conditions of isolation procedure were tested by automatic isolation procedure by ep Motion 5075 coupled with electrochemically detection at HMDE electrode to apply this procedure for the 3D chip microfluidic setup. The influence of four parameters (the way of HA–CdS complex preparation, concentration of glycan, interaction temperature and time of binding between glycan and HA–CdS) on the yield of the isolated CdS labeled viral protein was investigated.

Firstly, the influence of two preparation ways differing in the specific parameters (Section 2.4) on the isolation of HA–CdS complex was tested. Better way of preparation was confirmed for HA–CdS complex prepared by the second procedure, according to the result based on the detection of HA peak (Fig. 1A, blue color) as well as Cd peak (Fig. 1A, violet color).

Further, we aimed our attention at the optimization of the concentration of the glycan. Fig. 1B, blue color shows the dependence of Cd relative peak height on glycan concentration, and Fig. 1B, violet color shows the dependence of HA peak on the concentration of glycan. Changes in cadmium peak height showed the increasing dependence on the concentration of biotinylated

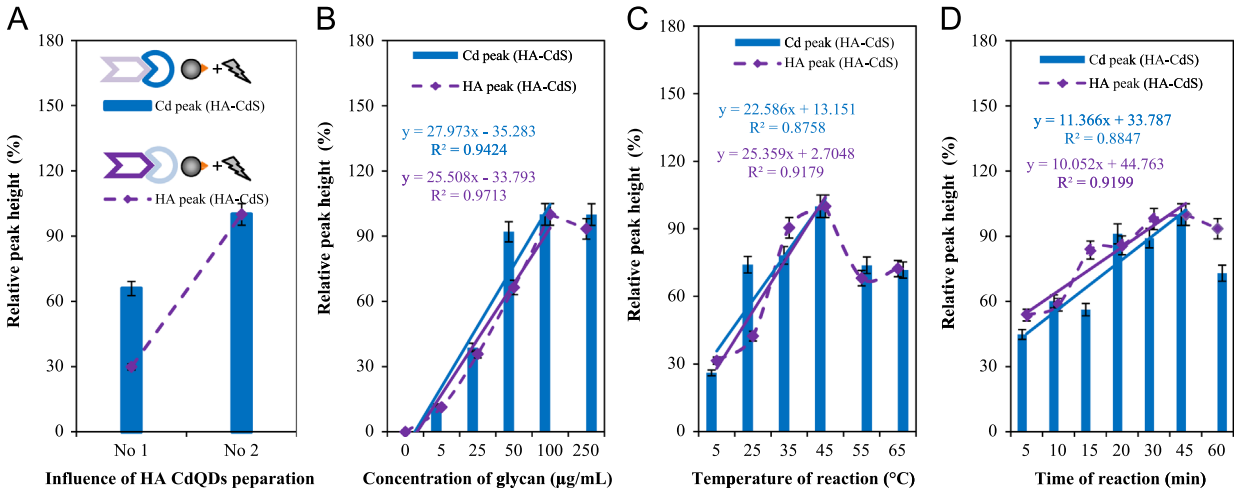

Fig. 1. Optimization of isolation procedure of HA–CdS complex by epMotion 5075 detected by electrochemical analysis of HA and Cd part of isolated HA–CdS complex. Cd peak was measured by DPASV. HA peak was measured by AdT DPV (for methods parameters see Section 2). Cd signal was described by columns and/or straight line and HA signal by points and/or dashed line. (**A**) Influence of the preparation way on detected signal of Cd and HA. (**B**) Influence of glycan concentration on detected signal of Cd and HA. (**C**) Influence of temperature on the linkage between glycan and HA–CdS. (**D**) Influence of reaction time on the linkage between glycan and HA–CdS. (For interpretation of the references to color in this figure legend, the reader is referred to the web version of this article.)

glycan, but only up to concentration of 50 μg/mL and this concentration was found as the optimal.

The further two optimized parameters (time and temperature of reaction) were directly connected with binding of glycan with HA–CdS. We tested six different values of temperature (5, 25, 35, 45, 55, and 65 °C) and seven different times of reaction (5, 10, 15, 20, 30, 45, and 60 min). Temperature of 45 °C was established as the best according to the Cd peak height (Fig. 1C, blue color) and HA peak (Fig. 1C, violet color). The highest effect of reaction time was observed for Cd peak (Fig. 1D, blue color) and HA peak (Fig. 1D, violet color) after 45 min of the incubation of glycan modified MPs with HA–CdS. If we summarize the results of the optimization, the best conditions were as it follows: concentration of glycan 50 μg/mL, preparation of HA–CdS complex by the second procedure, reaction time 45 min, and the reaction temperature 45 °C. These optimized conditions were applied for the 3D microfludic chip procedure.

3.3. Microfluidic analysis

Microfluidic devices have many advantages compared to their macro-scale counterparts, including a reduced reaction solution and cell consumption, an improved analysis speed, a greater portability, lower fabrication and operating costs, and the potential for parallel processing and integration with other miniaturized devices (Rios et al., 2012; Young, 1996). In this study we suggested, designed and fabricated the microfluidic device for the influenza detection (Fig. 2A). Optimized conditions for virus isolation were applied in the analysis process using 3D fabricated microfluidic chip. However, some further optimization steps aimed at chip detection parameters were done. The optimization of the electrochemical detection of Cd(II) under microfluidic conditions was the first step. Flow rate and time of accumulation were the optimized parameters. Sample was dosed by peristaltic pump in the operating range from 0 to 1200 μL/min (determined according to a flow number of peristaltic pump). With growing flow rate there was no enhancement in the yield of the isolation product over 480 μL/min (Fig. 2B). Between 134 and 480 μL/min there was the most efficient shift towards products detection and therefore the highest change of detected signal. The highest response of signal was achieved by the flow rate 480 μL/min (Fig. 2B). Thus, this optimized parameter was closely related to the next important parameter of electrochemical detection, time of accumulation. During the accumulation time there is a reaction between Cd and the surface of electrode, and due to the sensitivity of detection it was essential to test the effect of time of the accumulation on Cd peak height. Because the peak height did not markedly increase with higher time of accumulation of Cd (II), as the optimum 65 s was selected (Fig. 2C). Due to the fact that we obtained the optimal parameters for microfluidic device, it was possible to determine the accuracy. The system stability (including the isolation and detection process) was monitored (Fig. 2D) and Cd peak height was determined for five individual processes performed at five various chips. The presented error bars represent measurement error in the detection of the one specific isolation process. The accuracy of method was higher than 80 %. The influence of HA–CdS concentration (Cd concentration respectively) within the range from 0.06 to 0.5 mM on cadmium signal was investigated too. The increasing dependence in this concentration interval has parameters as it follows: $y=158.9x$, $R^2=0.9842$, $n=4$ (Fig. 2E) with RSD 5.2 %.

3.4. Application of suggested device to the influenza vaccine detection

Isolation and detection of influenza vaccine is introduced as a model of real sample detection in microfluidic device. Inactivated avian influenza viruses H5N1 labeled with CdS was isolated and detected by above-mentioned optimized procedure using 3D chip with three-electrode setup. For this experiment four equal samples and two negative controls were used. Each sample was used for the individual isolation and detection process. Electrochemical determination of the presence of formed HA–CdS complex by electrochemical quantification of cadmium(II) ions was used. The obtained results are shown in Fig. 3, where it is obvious the good accordance between samples and negative control, which gives no signal.

4. Conclusions

3D microfluidic chip was tested using CdS quantum dots labeled vaccine hemagglutinines. Our experiment demonstrated that the electrochemical analysis of isolated hemagglutinin using CdS quantum dots is very effective. Due to this fact, Cd signal has a great potential to become an alternative option as a rapid,

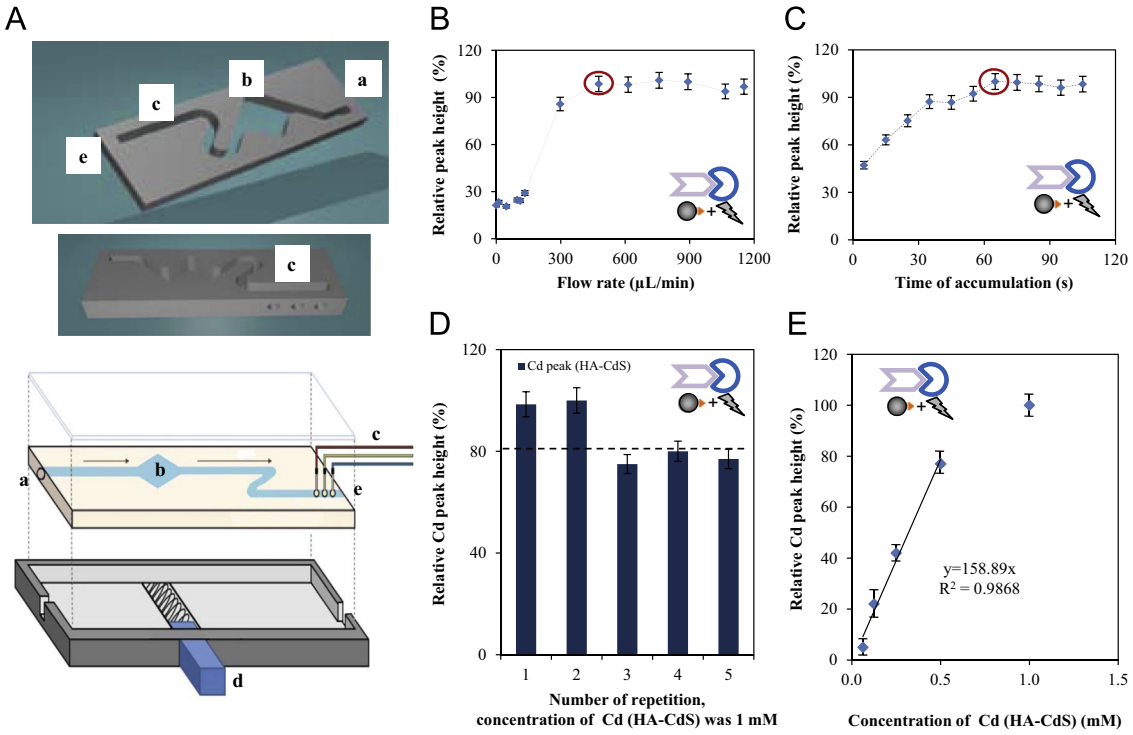

Fig. 2. (**A**) Scheme and model of 3D fabricated chip: (**a**) injection (influx) was used for dispensing the samples, buffer and electrolyte, (**b**) reaction cell, where whole process of isolation and magnetic pad, (d) was placed. (**c**) Three electrode setup, with working glassy carbon microelectrode, and efflux (**e**) for removing of reactants from the reaction chamber. Optimization of parameters for isolation and detection procedure. (**B**) Influence of flow rate (μL/min) on Cd relative peak height (%). (**C**) Dependence of relative peak height (%) on time of accumulation (s). (**D**) Dependence of relative Cd peak height (%) on concentration of Cd (HA–CdS) (1 mM). (**E**) Dependence of relative Cd peak height (%) on different concentration of Cd (HA–CdS). All measurements were provided by three electrode setup with working glassy carbon microelectrode. Differential pulse voltammetry (DPV) was a used for Cd signal detection (for methods parameters see Section 2).

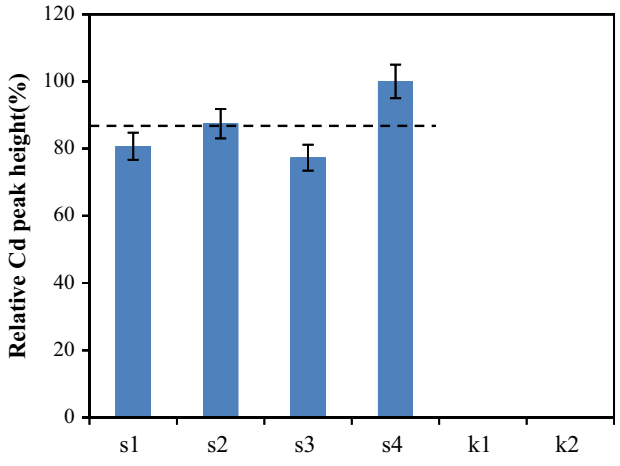

Fig. 3. Effect of isolation and detection procedure on the real sample detection. Real sample is inactivated avian influenza virus H5N1(295/Turkey/Canada/6213/66) labeled with CdS. The results were obtained through the electrochemical detection of Cd, using 3D chip. s1–s4 are the same samples and k1 and k2 are the negative controls.

sensitive, and specific detection of influenza hemagglutinin or influenza virus, and this 3D microfluidic system may be considered as a promising and powerful platform for the rapid diagnosis of influenza antigens and may be extended for diagnosis of other pathogens. As a future perspective, using of QDs with magnetic properties could be considered (Koole et al., 2009).

Acknowledgment

Financial support from CEITEC CZ.1.05/1.1.00/02.0068 and IGA IP16/2013 is highly acknowledged. We also thank to Assoc. Prof. Petr Lány from Department of Microbiology, Virology and Immunology, University of Veterinary and Pharmaceutical Sciences Brno for providing real sample of inactivated influenza.

Appendix A. Suppolementary material

Supplementary data associated with this article can be found in the online version at http://dx.doi.org/10.1016/j.bios.2013.10.031.

References

Bui, V.N., Ogawa, H., Ngo, L.H., Baatartsogt, T., Abao, L.N.B., Tamaki, S., Saito, K., Watanabe, Y., Runstadler, J., Imai, K., 2013. Arch. Virol. 158 (2), 451–455.
Casavant, B.P., Guckenberger, D.J., Berry, S.M., Tokar, J.T., Lang, J.M., Beebe, D.J., 2013. Lab Chip 13 (3), 391–396.
Chen, Q.J., Huang, S.P., Chen, J.J., Zhang, S.Q., Chen, Z., 2013. PLoS One 8 (1), 1–8.
Chou, T.C., Hsu, W., Wang, C.H., Chen, Y.J., Fang, J.M., 2011. J. Nanobiotechnol. 9, 1–13.
Epand, R.M., Epand, R.F., 2002. Biochem. J. 365, 841–848.
Garcia-Canas, V., Lorbetskie, B., Cyr, T.D., Hefford, M.A., Smith, S., Girard, M., 2010. Biologicals 38 (2), 294–302.
Gijs, M.A.M., 2004. Microfluid. Nanofluid. 1 (1), 22–40.
Hemmatzadeh, F., Sumarningsih, S., Tarigan, S., Indriani, R., Dharmayanti, N., Ebrahimie, E., Igniatovic, J., 2013. PLoS One 8 (2), 1–9.
Kamikawa, T.L., Mikolajczyk, M.G., Kennedy, M., Zhang, P., Wang, W., Scott, D.E., Alocilja, E.C., 2010. Biosens. Bioelectron. 26 (4), 1346–1352.
Kim, J.Y., Choi, K., Moon, D.I., Ahn, J.H., Park, T.J., Lee, S.Y., Choi, Y.K., 2013. Biosens. Bioelectron. 41, 867–870.
Koole, R., Mulder, W.J.M., van Schooneveld, M.M., Strijkers, G.J., Meijerink, A., Nicolay, K., 2009. Wiley Interdiscip. Rev.-Nanomed. Nanobiotechnol. 1 (5), 475–491.
Krasnoselsky, A.L., Katze, M.G., 2012. Nature 483 (7390), 416–417.
Krejcova, L., Dospivova, D., Ryvolova, M., Kopel, P., Hynek, D., Krizkova, S., Hubalek, J., Adam, V., Kizek, R., 2012. Electrophoresis 33 (21), 3195–3204.
Li, H., Shih, W.Y., Shih, W.H., 2007. Ind. Eng. Chem. Res. 46 (7), 2013–2019.
Lien, K.Y., Hung, L.Y., Huang, T.B., Tsai, Y.C., Lei, H.Y., Lee, G.B., 2011. Biosens. Bioelectron. 26 (9), 3900–3907.
Long, G.L., Winefordner, J.D., 1983. Anal. Chem. 55 (7), A712–A724.

Nejdl, L., Merlos, M.A.R., Kudr, J., Ruttkay-Nedecky, B., Konecna, M., Kopel, P., Zitka, O., Hubalek, J., Kizek, R., Adam, V., Electrophoresis. http://dx.doi.org/10.1002/elps.201300197, (inpress).
Polzin, C., Spath, S., Seitz, H., 2013. Rapid Prototyping J. 19 (1), 37–43.
Ramadan, Q., Gijs, M.A.M., 2012. Microfluid. Nanofluid. 13 (4), 529–542.
Rios, A., Zougagh, M., Avila, M., 2012. Anal. Chim. Acta 740, 1–11.
Shalyapina, A.Y., Zaporozhets, M.A., Volkov, V.V., Zhigalina, O.M., Nikolaichik, V.I., Gubin, S.P., Avilov, A.S., 2013. Russ. J. Inorg. Chem. 58 (1), 74–77.
Shembekar, N., Mallajosyula, V.V.A., Mishra, A., Yeolekar, L., Dhere, R., Kapre, S., Varadarajan, R., Gupta, S.K., 2013. PLoS One 8 (1), 1–13.
Schwarzer, J., Rapp, E., Hennig, R., Genzel, Y., Jordan, I., Sandig, V., Reichl, U., 2009. Vaccine 27 (32), 4325–4336.
Sochor, J., Hynek, D., Krejcova, L., Fabrik, I., Krizkova, S., Gumulec, J., Adam, V., Babula, P., Trnkova, L., Stiborova, M., Hubalek, J., Masarik, M., Binkova, H., Eckschlager, T., Kizek, R., 2012. Int. J. Electrochem. Sci. 7 (3), 2136–2152.
Stevens, J., Blixt, O., Tumpey, T.M., Taubenberger, J.K., Paulson, J.C., Wilson, I.A., 2006. Science 312 (5772), 404–410.
Suenaga, E., Mizuno, H., Penmetcha, K.K.R., 2012. Biosens. Bioelectron. 32 (1), 195–201.
Tong, S.X., Li, Y., Rivailler, P., Conrardy, C., Castillo, D.A.A., Chen, L.M., Recuenco, S., Ellison, J.A., Davis, C.T., York, I.A., Turmelle, A.S., Moran, D., Rogers, S., Shi, M., Tao, Y., Weil, M.R., Tang, K., Rowe, L.A., Sammons, S., Xu, X.Y., Frace, M., Lindblade, K.A., Cox, N.J., Anderson, L.J., Rupprecht, C.E., Donis, R.O., 2012. Proc. Natl. Acad. Sci. USA 109 (11), 4269–4274.
Tsai, S.S.H., Wexler, J.S., Wan, J.D., Stone, H.A., 2013. Lab Chip 13 (1), 119–125.
Vyslouzilova, L., Krizkova, S., Anyz, J., Hynek, D., Hrabeta, J., Kruseova, J., Eckschlager, T., Adam, V., Stepankova, O., Kizek, R., 2013. Electrophoresis 34 (11), 1637–1648.
Xu, Y.H., Wang, E.K., 2012. Electrochim. Acta 84, 62–73.
Young, J., 1996. Forbes 158 (7), 210–211.